

Optimization of Microstructure Development: Application to Hot Metal Extrusion

E.A. Medina, S. Venugopal, W.G. Frazier, S. Medeiros, W.M. Mullins, A. Chaudhary, R.D. Irwin, R. Srinivasan, and J.C. Malas

A new process design method for controlling microstructure development during hot metal deformation processes is presented. This approach is based on modern control theory and involves state-space models for describing the material behavior and the mechanics of the process. The challenge of effectively controlling the values and distribution of important microstructural features can now be systematically formulated and solved in terms of an optimal control problem. This method has been applied to the optimization of grain size and certain process parameters such as die geometry profile and ram velocity during extrusion of plain carbon steel. Various case studies have been investigated, and experimental results show good agreement with those predicted in the design stage.

Keywords

die design, dynamic recrystallization, extrusion, microstructure modeling, optimal control theory, process design

1. Introduction

DEVELOPMENT OF optimal design and control methods for manufacturing processes is needed for effectively reducing part cost, improving part delivery schedules, and producing specified part quality on a repeatable basis. Existing design methods are generally ad hoc and cannot be used to evaluate the effects of primary process parameters such as deformation rates, die and workpiece temperatures, and tooling system configuration on the manufacturing process and on the final product. This situation presents major challenges to process engineers who are faced with ever-increasing constraints on cost and quality and growing production requirements for near net-shape components with controlled microstructures and properties. It is important to develop new systematic methodologies for process design and control based upon scientific principles which sufficiently consider the behavior of the workpiece material and the mechanics of the manufacturing process.

This paper presents a new strategy for systematically calculating near-optimal control parameters for hot metal deformation processes. This approach is based on modern control theory (Ref 1) and involves developing state-space models for material behavior and hot deformation processes. In this strategy, control system design is carried out in two basic stages. Analysis and optimization are performed in both stages. In the first stage, the kinetics of certain dynamic microstructural phenomena and the intrinsic hot workability of the metal alloy system are used, along with an appropriately chosen optimality criterion, to calculate nominal strain, strain rate, and temperature trajectories (histories) that will cause the microstructure at

a given location in a workpiece to evolve from its initial state, through an acceptable path, to the desired final state. These nominal trajectories are valid for different hot deformation processes (forging, rolling, extrusion, etc.), and they are thus independent of die geometry and flow pattern. A suitable process simulation model, which could range from a simple slab-type model to a high-fidelity finite element simulation model, is then used in the second stage to calculate the process control parameters, such as ram velocity profiles and billet temperature, which best achieve, in selected areas of the workpiece, the nominal strain, strain rate, and temperature trajectories calculated in the first stage.

An application of the new process design approach to a round-to-round hot metal extrusion process is investigated in this paper. An extrusion process was selected for study for the following reasons: extrusion typically involves large deformation with large variations in strain rate; relatively simple analytical models are available for describing the process; and strain and strain-rate trajectories can be effectively controlled via optimized design of die geometry. The following sections present the development of the two-stage optimal design approach, along with its application to the design of an extrusion process. Case studies and an experimental validation of the procedure are also presented.

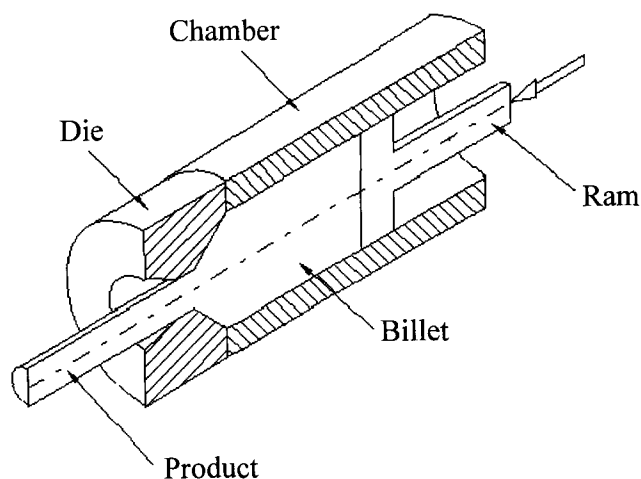


Fig. 1 The extrusion process

E.A. Medina, S. Venugopal, W.G. Frazier, S. Medeiros, W.M. Mullins, A. Chaudhary, and J.C. Malas, Wright Laboratory, WL/MLIM, Wright-Patterson AFB, Ohio 45433, USA; R.D. Irwin, School of Electrical Engineering and Computer Science, Ohio University, Athens, Ohio 45701, USA; and R. Srinivasan, Mechanical and Materials Engineering Dept., Wright State University, Dayton, Ohio 45435, USA.

1.1 Description of Direct Extrusion

Extrusion is a process by which the cross section of a billet is reduced by forcing it to flow through a die. In a typical direct extrusion process, shown in Fig. 1, a billet is placed in a chamber and the force exerted by the ram makes the metal flow through the die. The process is used to manufacture both finished and semifinished products. As a primary processing operation, extrusion is used to refine the large-grain cast structure. The extruded product is then in a condition more amenable to final shape making by other metal forming operations. The refinement of grains during extrusion is influenced by several factors, including the initial temperature of the billet, the reduction in area, and the strain-rate variations that the material experiences during deformation.

Hot extrusion is usually carried out using converging dies, in which the cross section of the die orifice changes gradually from the initial billet shape to the final product shape over the length of the die. The strain and strain-rate variations that the material experiences as it flows through the die depend on the die profile. Conical die, constant-strain-rate die, and cubic streamline die are examples of die configurations commonly used in industry.

1.2 Microstructural Evolution during Hot Deformation

Microstructural changes which occur during hot deformation are consequences of complex metallurgical phenomena such as recovery, recrystallization, grain growth, phase transformations, and precipitation and dissolution reactions. These phenomena may occur dynamically during hot deformation processing or statically during post-deformation cooling or heat treatment. The mechanisms and kinetics of these phenomena, as well as the associated changes in size, morphology, distribution, volume fraction, and composition of the constituent phases, are strongly dictated by the macroscopic heat flow and material flow processes. While the temperature distribution in the workpiece is controlled primarily by the interface heat transfer between the workpiece and the dies, frictional heating and deformation heating effects also contribute significantly. At the same time, the distributions of strain, strain rate, effective stress, and hydrostatic stress within the deforming body are

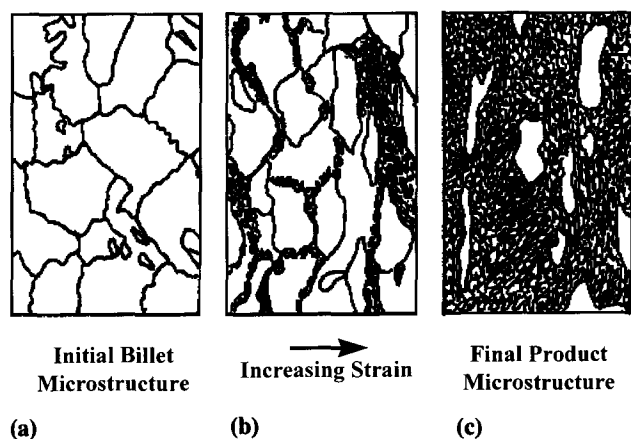


Fig. 2 Schematic representation of the progression of dynamic recrystallization with strain. (a) Initial billet microstructure. (b) Intermediate microstructure. (c) Final product microstructure

influenced by the material flow behavior as well as the thermal history.

Dynamic recrystallization is commonly observed in hot extrusion processes which involve very large strains (typically the true plastic strain, ϵ , is greater than 0.5). Metals and alloys characterized by relatively low stacking-fault energy (e.g., copper, nickel, austenitic steels) have a high propensity for undergoing restoration via dynamic recrystallization. Under hot-working conditions, these materials exhibit flow curves containing single maxima. A schematic representation of a typical microstructure evolution during dynamic recrystallization is shown in Fig. 2. When the plastic strain exceeds a critical value, ϵ_c , dynamically recrystallized grains nucleate. Additional deformation results in a replacement of the unrecrystallized structure by a completely recrystallized structure. This transition from unrecrystallized to recrystallized microstructure is strongly dependent on processing conditions and may occur over a relatively small increment in deformation.

2. The Two-Stage Approach to Optimal Control of Deformation Processes

The process design and control strategy presented in this paper requires three basic components for defining and setting up the optimization problem: a dynamical system model, physical constraints, and an optimality criterion. In metal forming, the system models of interest are material behavior and deformation process models; constraints include the hot workability of the workpiece and the limitations of the forming equipment. Optimality criteria could be related to achieving a particular final microstructure, regulating temperature, and/or maximizing deformation speeds.

The present two-stage approach separates analysis and optimization into a workpiece material behavior control problem and a process mechanics control problem. Since optimization methods are used in both design stages, the two stages are also called *microstructure development optimization* and *process optimization* in the block diagram of Fig. 3. The microstructure development optimization determines optimal trajectories of strain, $\epsilon(t)$; strain rate, $\dot{\epsilon}(t)$; and temperature, $T(t)$. From these optimal material trajectories, the process optimization stage determines optimal process control parameters: the die shape; the ram velocity profile, $V_{\text{ram}}(t)$; and the billet temperature $T_{\text{billet}}(t)$. The goals of the first stage are to achieve enhanced workability and to obtain prescribed microstructural features in the deformed workpiece. In the second stage, a primary goal is to achieve the thermomechanical conditions obtained from stage one for predetermined regions of the deforming workpiece. It is recognized that this two-stage approach yields idealized process control solutions that could be further improved with advanced feedback methods.

2.1 Material Behavior and Process Modeling Issues

The effectiveness of the two-stage approach presented in this paper is largely dependent on the availability and reliability of models for the behavior of the material and for the metal forming process. In the first stage, material behavior models that describe the kinetics of primary metallurgical mecha-

nisms, such as dynamic recovery, dynamic recrystallization, and grain growth during hot working, are required for analysis and optimization of material system dynamics. These mechanisms have been studied extensively for a wide range of metals and alloys (Ref 2-5). The relationships for describing particular microstructural processes have been developed and reported for conventional materials such as aluminum, copper, iron, nickel, and their dilute alloys, with steel receiving the most study. It has also been suggested that for certain ranges of temperature and strain rate, the deformation mechanisms of specialty alloys, such as superalloys, intermetallics, ordered alloys, and metal-matrix composites, become well defined and are amenable to modeling (Ref 6, 7).

As an illustration of a material behavior model, consider the case of a material that undergoes dynamic recrystallization during hot deformation. A possible state-space model is given by:

$$\begin{bmatrix} \dot{d} \\ \dot{\chi} \\ \dot{\epsilon} \\ \dot{T} \end{bmatrix} = \begin{bmatrix} f_1(T, \dot{\epsilon}, d) \\ f_2(T, \dot{\epsilon}, d, \chi) \\ u \\ \frac{\eta \sigma \dot{\epsilon}}{\rho C_p} \end{bmatrix} \quad (\text{Eq 1})$$

where d is grain size, χ is percent recrystallized, f_1 and f_2 are prespecified functions, u is the system input, η is a coefficient that determines how much work is converted into heat, σ is flow stress, ρ is the density, and C_p is the heat capacity of the material. Note that the system input, u , is the strain-rate for this model. The trajectories followed by the state variables d , χ , ϵ , and T , which are dictated by their initial conditions and by the trajectory followed by the system input (in this case the strain rate), determine the evolution of the material microstructure during deformation.

In several industries, process modeling has reached a high level of sophistication and acceptance as a process analysis tool. Current process models are capable of analyzing fairly complex material flow operations such as three-dimensional, non-isothermal deformation processes with a sufficiently high degree of accuracy. For example, in the

forging industry, detailed numerical analyses of the phenomenon of the workpiece filling the forging die, the resulting die stresses, and the post-deformation heat treatment of the workpiece are applied for verification of forging and heat treatment process designs (Ref 8, 9).

2.2 Material Behavior Constraints and Optimality Criterion

In addition to dynamic system models, the formulation of an optimal control problem requires a statement of physical constraints and specification of an optimality criterion. The limiting process conditions for acceptable hot workability are important material behavior constraints in the first stage of the control strategy. Several methods for identifying acceptable strain rate and temperature ranges for hot working metal alloys have been presented in scientific literature: material flow stability analysis (Ref 6, 7), deformation maps (Ref 8), and damage nucleation maps (Ref 9). Within the acceptable processing regime of temperature and strain-rate variations, a particular thermomechanical trajectory is determined using the prescribed optimality criterion, such as producing specified hot-worked microstructural characteristics.

2.3 General Formulation of the Optimal Control Problem

Following the description above, the design problem is formulated here into an open-loop optimal control problem that can be stated as follows: Find u to minimize the optimality criterion

$$J = h(x(t_f)) + \int_0^{t_f} g(x(t), u(t)) dt \quad (\text{Eq 2})$$

while satisfying the system state equation

$$\dot{x}(t) = f(x(t), u(t)), \quad x(0) = x_0 \quad (\text{Eq 3})$$

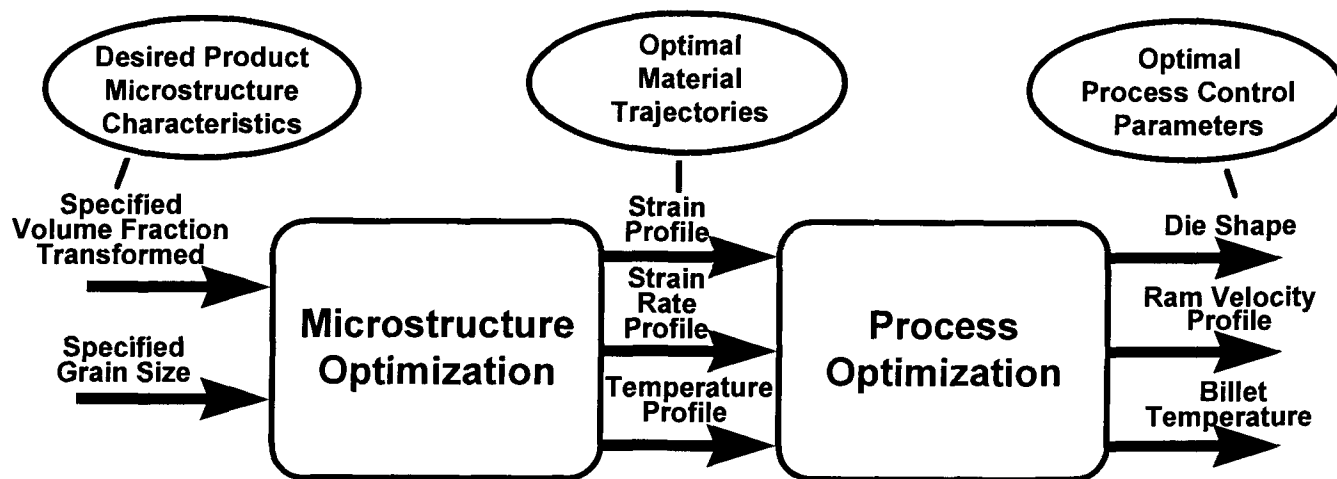


Fig. 3 Block diagram of the two-stage approach

where t is time, $x(t)$ is a vector of state variables, t_f is the final time for the complete deformation process, h is a penalty function associated with violating the desired final state, g is the integrand of the penalty associated with the trajectories followed by the state variables and the input, f is a vector function that describes the process dynamics, and x_0 is the initial state vector. In this context, the term *final state* or *final value* refers to the value of the state vector or the variable of interest at the end of processing, while the term *trajectory* refers to a history of the values attained by the variable under consideration during processing.

2.4 Optimality Criteria for Microstructure Development

Careful selection of optimality criteria is a crucial task for finding the most appropriate design solutions. In the control of microstructure development during hot-metal deformation, design criteria include the requirement of producing specified microstructural features and/or gradient of microstructure within a given variance on a repeatable basis. These objectives and others can usually be formulated as functions to be minimized, and they are often lumped together into a single scalar optimality criterion J in the form

$$J = J_1^F + J_2^F + \dots + J_{n_F}^F + J_1^T + J_2^T \dots + J_{n_T}^T \quad (\text{Eq 4})$$

where the superscripts F and T refer to requirements on desired final states and trajectories, respectively, and n_F and n_T refer to the total numbers of such specifications. In the case where it is desired that microstructure feature x achieve a value of x_d at the termination of the deformation process, the corresponding term in J often has the form

$$J_i^F = \beta_i (x(t_f) - x_d)^2 \quad (\text{Eq 5})$$

where β_i is a weighting factor. This type of function can also be used to include certain fixed process parameters and other val-

ues for non-microstructural quantities, such as strain and temperature, in the optimization calculations. The terms J_j^T in the optimality criterion define requirements on the trajectories followed by the state variables and control inputs during the forming process, and they have integral forms.

Table 1 shows some typical optimality criteria for microstructure development during hot deformation. Both final value and trajectory specifications have been included. The general formulation of this approach allows new terms to be defined according to the specific needs of each design problem. The quantities $f(x, a)$ and $f(x, a, b)$ in Table 1 are penalty functions that can be used to constrain optimized design solutions to stay within acceptable process parameter ranges for satisfactory material workability or to stay within the capabilities of the forming equipment. These functions evaluate to virtually zero for values of x in the acceptable range and attain very high values when x is outside that range. Scalars a and b define the acceptable ranges for process parameters such as temperature or strain rate. An example of a penalty function is shown in Figure 4.

The weighting factors β_j serve three purposes: (a) they are used to scale various J -terms so that they have comparable influence in the overall optimality criterion; (b) they are increased for certain J -terms according to their relative importance to achieving overall design requirements; and (c) they may be adjusted in order to avoid possible conflicts in design requirements and obtain a satisfactory compromise solution.

2.5 Solution of the Microstructure Development Trajectory Optimization Problem

The approach used in obtaining a solution to the optimization problem described above depends on two developments. First, a set of necessary conditions for optimality is obtained by applying variational calculus principles (Ref 1); this formulation transforms the optimization problem to a problem of solving a set of constraint equations. Next, a search-based numerical algorithm is developed for the solution of these equations. Details of the algorithm formulation are given by Frazier (Ref 10).

Table 1 Examples of typical terms for the optimality criterion for microstructure development during hot metal deformation

Design objective	Term in the optimization criterion
Achieve final average grain size x_d	$J_i^F = \beta_i (x(t_f) - x_d)^2$
Achieve final strain of ϵ_1	$J_i^F = \beta_i (x(t_f) - \epsilon_1)^2$
Maintain strain rate between u_1 and u_2 because of workability considerations	$J_j^T = \int_0^{t_f} \beta_j(t) f(u, u_1, u_2) dt$
Limit deformation heating; initial temperature is T_0	$J_j^T = \int_0^{t_f} \beta_j(t) (T - T_0)^2 dt$
Keep strain rate under u_1 because of equipment limitations	$J_j^T = \int_0^{t_f} \beta_j(t) f(u, u_1) dt$
Maintain temperature between T_1 and T_2 because of workability considerations	$J_j^T = \int_0^{t_f} \beta_j(t) f(T, T_1, T_2) dt$
Limit energy consumption; $u^2(t)$ is a measure of power	$J_j^T = \int_0^{t_f} \beta_j(t) u^2(t) dt$

3. Application of the Two-Stage Optimization to Steel Extrusion

Results of the application of the two-stage approach to the optimization of a steel extrusion process are presented in this section. A state-space model for microstructural response was formulated from available microstructural models. The optimization algorithm was then applied to obtain controlled grain sizes through hot extrusion of plain carbon steel.

3.1 Models for Dynamic Recrystallization of Steel

The application of the proposed microstructure development optimization approach depends on the existence of a state-space model that describes how the microstructure changes in time as a function of various process parameters. Microstructural evolution during hot deformation of steel can be described in terms of changes in quantities such as grain size

and volume fraction transformed as functions of process parameters such as strain, strain rate, and temperature. Many such descriptions for hot deformation of steel have been developed and have been summarized by Kumar et al. (Ref 11). This study used a model developed by Yada et al. (Ref 12-14) to describe the effects of strain, strain rate, and temperature on the microstructural changes during hot rolling of steel. According to this model, the volume fraction recrystallized, χ , evolves according to the expression

$$\chi = 1 - \exp \left(\ln(2) \left(\frac{(\epsilon - \epsilon_c)^2}{\epsilon_{0.5}} \right) \right) \quad (\text{Eq 6})$$

where

$$\begin{aligned} \epsilon_c &= 4.76 \times 10^{-4} \exp(8000/T) \\ \epsilon_{0.5} &= 1.144 \times 10^{-5} d_0^{0.28} (\dot{\epsilon})^{0.05} \exp(6240/T) \end{aligned} \quad (\text{Eq 7})$$

Note that χ is primarily dependent on the imposed strain, ϵ . The volume fraction recrystallized is essentially zero until a critical value of strain, ϵ_c . Beyond this strain, recrystallization proceeds rapidly along an S-curve; complete recrystallization occurs with very little additional deformation. The kinetics of the recrystallization are described by the amount of additional strain required to cause 50% recrystallization ($\epsilon_{0.5}$). In Eq 7, $\epsilon_{0.5}$ is very small and complete recrystallization occurs almost instantaneously after the critical strain. The volume fraction recrystallized also depends upon strain rate $\dot{\epsilon}$, temperature T , and initial grain size d_0 , through their influence on ϵ_c and $\epsilon_{0.5}$. However, this dependence is negligible. The average grain size d obtained after recrystallization is given, as a function of only strain rate and temperature, by:

$$d = 22,600 (\dot{\epsilon})^{-0.27} \exp \left(-0.27 \frac{Q}{RT} \right) \quad (\text{Eq 8})$$

where $Q = 267$ kJ/mol, the activation energy, and R is the universal gas constant. Equations 6 and 8 were developed for deformation at constant strain rate and temperature.

These equations imply that complete recrystallization occurs instantaneously. Furthermore, since grain size depends upon strain rate, temperature, and prior grain size, each recrystallization step will result in changes in average recrystallized grain size, which will depend upon the current deformation conditions.

In order to transform Eq 6 into a form that can be used in the state equation framework, it is assumed that χ is not sensitive to the rate of change of strain rate or the rate of change of temperature. The chain rule of differentiation can then be applied to Eq 6 to obtain:

$$\dot{\chi} = \frac{\partial \chi}{\partial \epsilon} \frac{\partial \epsilon}{\partial t} = \frac{\partial \chi}{\partial \epsilon} \dot{\epsilon} = \frac{2 \ln 2}{\epsilon_{0.5}^2} (\epsilon - \epsilon_c)(1 - \chi) \dot{\epsilon} \quad (\text{Eq 9})$$

which is a dynamic equation for the time derivative of the volume fraction recrystallized. This equation is correct to first order.

During deformation, most of the mechanical work exerted on the workpiece transforms into heat, and this results in an increase in temperature. The equation for the rate of change of temperature due to deformation can be easily shown to be:

$$\dot{T} = \frac{\eta \sigma \dot{\epsilon}}{\rho C_p} \quad (\text{Eq 10})$$

where the flow stress σ is a function of strain, strain rate, and temperature given by (Ref 13):

$$\begin{aligned} \sigma &= \sinh^{-1}[(\dot{\epsilon}/A)^{(1/n)} \exp(Q/RT)] / 1.15 \times 10^{-5} \text{ kPa} \\ \ln A &= 13.92 + 9.023/\epsilon^{0.502} \\ n &= -0.97 + 3.787/\epsilon^{0.368} \\ Q &= 125 + 133.3/\epsilon^{0.393} \text{ kJ/mol} \end{aligned} \quad (\text{Eq 11})$$

In Eq 10, η is the fraction of mechanical work converted to heat and is generally about $1/1 + m$, where m is the strain-rate sensitivity of the workpiece material (Ref 6).

The state-space model for the chosen steel, which gives the evolution in time of χ , ϵ , and T can be summarized as:

$$\begin{bmatrix} \dot{\chi} \\ \dot{\epsilon} \\ \dot{T} \end{bmatrix} = \begin{bmatrix} \frac{2 \ln 2}{\epsilon_{0.5}^2} (\epsilon - \epsilon_c)(1 - \chi) \dot{\epsilon} \\ u \\ \frac{\eta \sigma u}{\rho C_p} \end{bmatrix} \quad (\text{Eq 12})$$

$$d = 22,600 u^{-0.27} e^{-0.27Q/RT} \quad (\text{Eq 13})$$

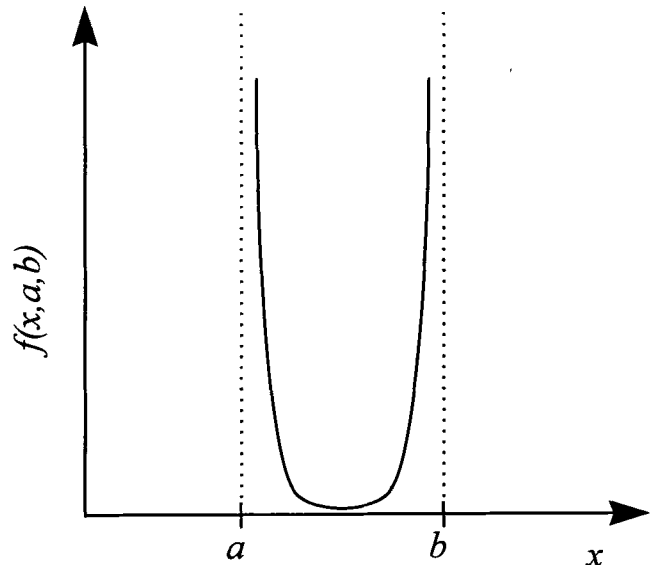


Fig. 4 Penalty function ($f(x, a, b)$) for constraining process parameters between a and b

As mentioned above, the evolution of strain is completely determined by the strain rate, which is the system input, i.e., $u = \dot{\epsilon}$. The average grain size after recrystallization given in Eq 13, which is the same as Eq 8, is treated as an output of the dynamical system in the sense that it does not influence the evolution of ϵ , T , or χ , and therefore it does not need to be included as one of the state variables.

3.2 Stage One: Formulation of a Cost Functional and Trajectory Optimization

Since the microstructure of a material directly influences its mechanical properties, control of microstructural features is of primary concern in the design of deformation processes. Therefore, the cost function should emphasize the final microstructural state of the material. In addition, it is also important that the path followed by the material during the deformation process remain within certain bounds to prevent undesirable events. Unacceptable designs may be due to failure of the material (e.g., cracking can occur if the process is not designed to stay within ranges of acceptable material workability). It would also be unacceptable to calculate material trajectories that cannot be obtained in practice because of limitations in the capacity of the equipment. By including material and equipment limitations into the optimality criterion, these difficulties can be prevented. Table 1 lists several types of terms that can be included in the optimality criterion to account for design constraints.

For the extrusion case studied in this effort, the optimality criterion was formulated so as to attain a final strain of 2.0, while maintaining the average recrystallized grain size at a desired value of 26 μm throughout the process. With these requirements, the optimality criterion is given by:

$$J = 10(\epsilon(t_f) - 2.0)^2 + \int_0^{t_f} (d(t) - 26)^2 dt \quad (\text{Eq 14})$$

The weighting factor of 10 for the term that penalizes deviations from the desired final strain was selected by comparing the results of several trials in which different weights were used.

The trajectory optimization algorithm was successfully applied to this problem, and the results are presented in the solid lines marked as case 1 in Fig. 5 to 7. These figures show the optimal strain rate, temperature, and strain trajectories. Figure 8 shows the corresponding change in recrystallized grain size, as predicted by the model. The initial grain size for the material was approximately 180 μm . The solid vertical line at the beginning of the average grain size trajectory corresponds to the change in grain size which occurs when the first recrystallization takes place at a strain of approximately 0.25. Figures 5 to 8 also show additional optimal design cases for desired final grain sizes of 30 μm (case 2) and 15 μm (case 3). The initial temperature for case 1 and 2 was 1273 K; for case 3 it was 1223 K. Figures 7 and 8 show that the desired recrystallized grain size trajectory and final strain are obtained in all three cases.

3.3 Stage Two: Process Mechanics Control and Optimal Die Design

In a metal forming operation, the trajectories of the various parameters (i.e., strain, strain rate, temperature, etc.) that influence microstructure are the result of the combined effects of all deformation process parameters, such as the die and workpiece geometry, die and workpiece temperatures, and ram velocity. The second stage of the optimal design problem involves identifying the process parameters that can deliver the desired trajectories identified in the first stage. Generally, not all points in the deforming piece will follow the same strain, strain rate, and temperature trajectories. Therefore, the deformation process parameters may have to be designed in order to ensure that selected critical areas of the workpiece experience the designed trajectories. In principle, a second optimization problem can be formulated that determines values for process parameters to achieve the desired trajectories at predetermined points in the workpiece. Such an approach would require a simulation of the deformation process (by slab analysis, finite element modeling, etc.) for each evaluation of the objective function.

In this paper, extrusion has been chosen as the deformation process. For a round-to-round extrusion, it is possible to analytically calculate the die shape and ram velocity necessary for achieving the desired strain and strain-rate profiles at the center line of the workpiece, using slab analysis. If r_0 is the initial radius of a cylindrical billet, L is the die length, and t_f is the time required by a slab of material to traverse the length of the die, the ram velocity can be computed from the strain trajectory $\epsilon(t)$ as:

$$V_{\text{ram}} = \frac{L}{\int_0^{t_f} (\exp \epsilon(t)) dt} \quad (\text{Eq 15})$$

The shape of the die, expressed as radius r and axial position y , for different locations along the strain trajectory can be calculated as:

$$\begin{aligned} r(t) &= r_0 \exp(-\epsilon(t)/2) \\ y(t) &= V_{\text{ram}} \int_0^t \exp(\epsilon(\tau)) d\tau \end{aligned} \quad (\text{Eq 16})$$

The optimal die profiles shown in Fig. 9 were obtained by using this approach. The corresponding ram velocities are 8.43 mm/s for case 1, 5.0 mm/s for case 2, and 25.1 mm/s for case 3. The die shapes for the three cases discussed are almost coincident. Since the die shape is almost the same for the three optimization cases considered, one can achieve different recrystallized grain sizes simply by changing the velocity of the extrusion ram and the initial billet temperature. The three optimal die shapes are almost identical to that of the constant-strain-rate die.

3.4 Comparison with Standard Die Designs

In addition to the three optimal design cases discussed above, Fig. 5 to 8 show the trajectories of the strain, strain-rate,

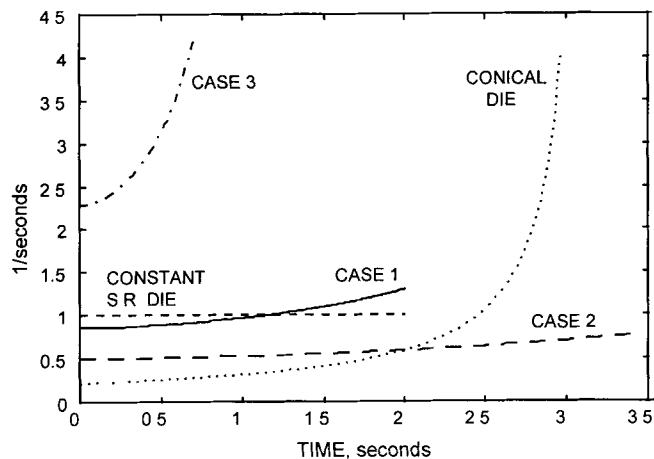


Fig. 5 Strain rate trajectories

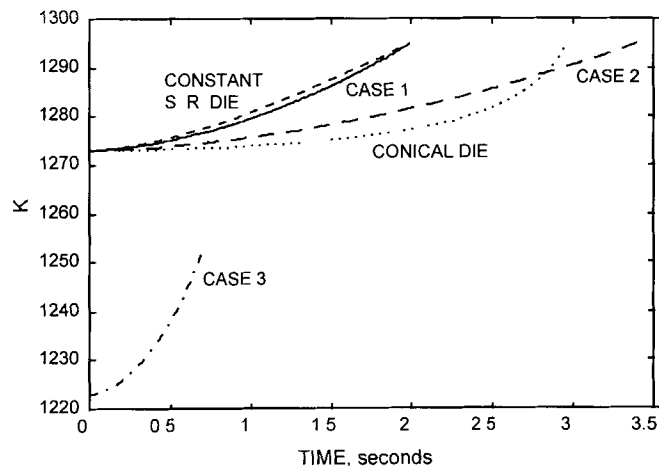


Fig. 6 Temperature trajectories

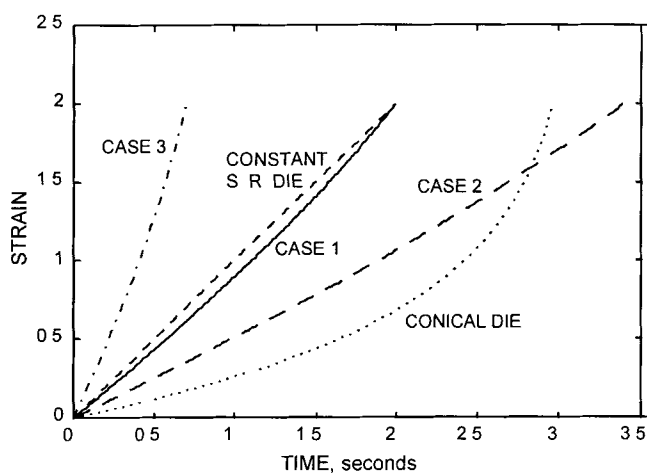


Fig. 7 Strain trajectories

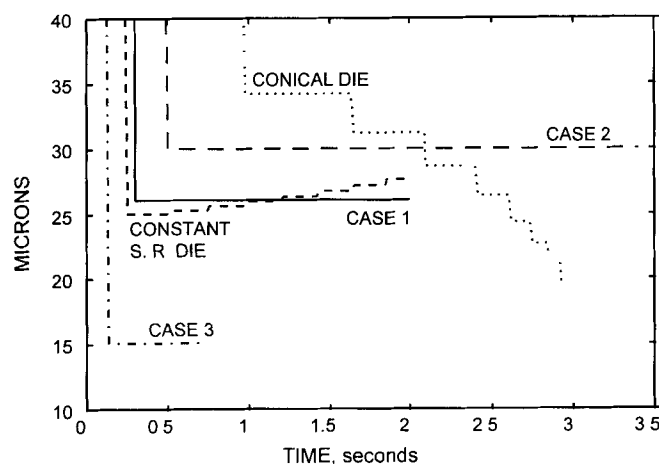


Fig. 8 Recrystallized grain size trajectories

temperature, and recrystallized grain size for two standard converging dies: the conical die and the constant-strain-rate (CSR) die. The profiles of these standard dies are included in Fig. 9. Both these dies result in the same final strain of 2.0, but the trajectories are quite different. The CSR die, as the name suggests, maintains a constant strain rate throughout the length of the die, while the strain rate experienced by the workpiece during extrusion through a conical die starts at a very low value at the beginning of extrusion and increases by almost one order of magnitude at the end (Fig. 5). The plots assume a ram velocity of 8.43 and 8.0 mm/s for the CSR and conical dies, respectively. In Fig. 8, the recrystallized grain size trajectories for these two die shapes show step changes that correspond to successive dynamic recrystallizations.

The strain rate using the die in case 1 begins slightly below that for the CSR die, but it increases to a value slightly higher than that for the CSR die by the end of extrusion. Figure 6 shows that the temperature rise for the CSR die is equal to that for case 1, while Fig. 8 shows that the final recrystallized grain size for the CSR die is slightly larger than that for case 1. These observations can be rationalized as follows. According to Eq 8, the final recrystallized grain size is influenced by two factors:

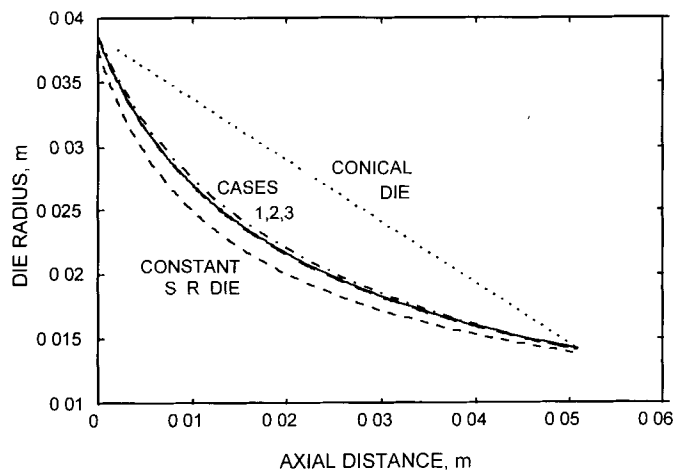
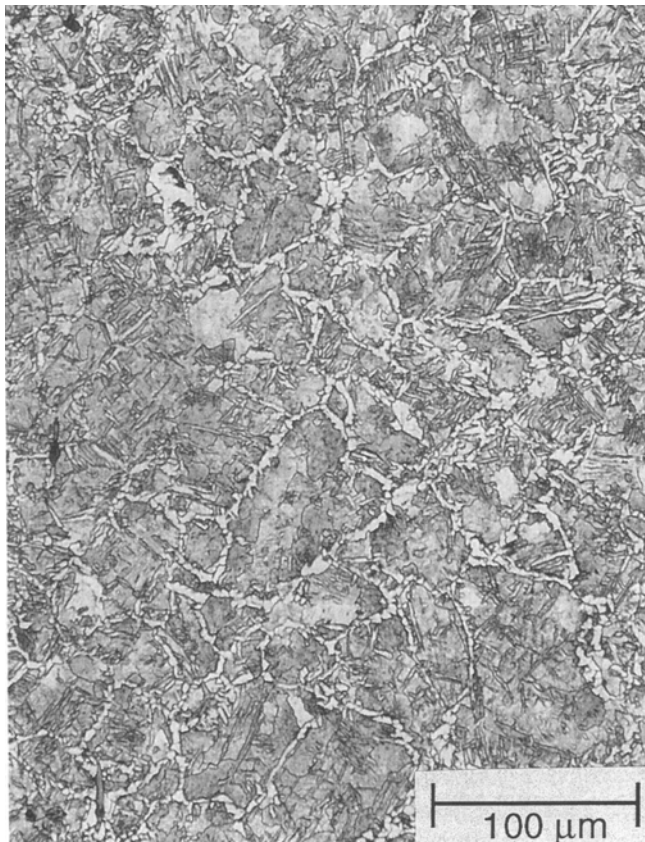
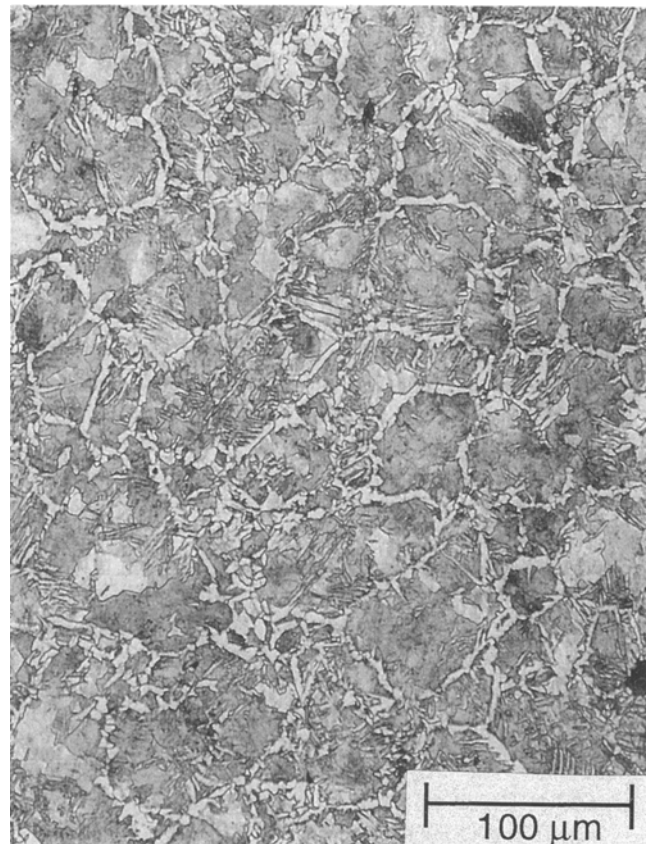


Fig. 9 Die profiles

the temperature and the strain rate. Under isothermal conditions, at a constant strain rate, the recrystallized grain size will be constant once the critical strain is exceeded. However, during any deformation process, some increase in temperature occurs due to the conversion of mechanical work into heat. At a



(a)



(b)

Fig. 10 Microstructures at location of (first) critical strain and die exit

constant strain rate, this results in a gradual increase in recrystallized grain size with each successive recrystallization. This increase in recrystallized grain size is seen as steps in the grain size trajectory for the CSR die in Fig. 8. The die designed in case 1 compensates for this increase in recrystallized grain size by gradually increasing the strain rate, as seen in Fig. 5. The result is the constant recrystallized grain size of 26 μm seen in Fig. 8. In the case of the conical die there is also an increase in temperature due to deformation heating, but the simultaneous increase in strain rate is substantially greater. As a result of this, the recrystallized grain size decreases with each successive recrystallization.

4. Validation of the Two-Stage Design Approach

An extrusion die with the shape obtained from case 1 of the trajectory optimization algorithm was fabricated from H-13 tool steel. A billet of AISI 1030 steel was extruded with a 6000 kN Lombard horizontal extrusion press located at Wright-Patterson Air Force Base, Ohio. The initial temperature of the billet was 1273 K and that of the extrusion chamber, die, and follower block was 533 K. A ram velocity of 8.43 mm/sec was used. Under these conditions, the resultant grain size in the extruded workpiece would be 26 μm , as determined in case 1. The extrusion was interrupted when the billet had only partially ex-

truded through the die. The billet was subsequently removed from the tooling and water quenched. Between the end of extrusion and the beginning of quench 39 seconds elapsed.

The partially extruded billet was sectioned along a diametral plane and prepared for metallographic examination. The specimen was etched with 2% nital to reveal grain boundaries for grain size measurements. The grain sizes at different locations along the centerline of the workpiece in the deformation zone were measured using the Heyn intercept method (Ref 15). The observed grain size was the result of dynamic recrystallization during extrusion and any grain growth that may have occurred during the 39 second transfer time. Figure 10 shows typical microstructures from the partially extruded billet. The experimentally measured grain sizes are shown in Figure 11. Clearly, the measured grain size was larger than the predicted grain size of 26 μm . Therefore, an attempt was made to take into account any grain growth that may have occurred during the transfer time.

This extrusion experiment was simulated using the finite element simulation program ANTARES (Ref 16). The billet and die domains were discretized to an average mesh size of 3 mm square. The finite element simulation was performed using an individual step increment approximately equal to $1/100$ of the total ram stroke. The process was simulated for the nonlinear coupled response of the billet and the thermal response of the die. After the partial extrusion, the temperature at the billet cen-

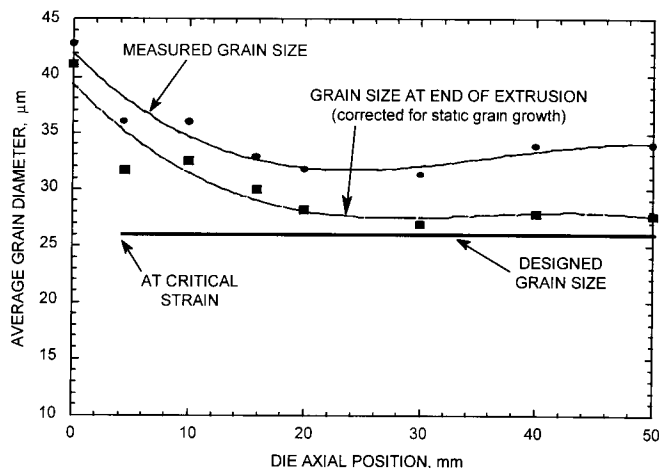


Fig. 11 Measured and corrected prior-austenite grain size versus position along die centerline

terline increased to 1313 K due to deformation heating. The cooling of the partially extruded billet for 39 s was then simulated. Figure 12 shows the resultant evolution in temperature along the billet centerline. Based on this evolution of temperature and the experimentally measured grain size, the grain size variation along the billet centerline was calculated using the equation (Ref 14)

$$d^2 = d_0^2 + A \exp \left(\frac{-Q_{gg}}{RT} \right) \quad (\text{Eq 17})$$

where $A = 1.44 \times 10^{12} (\mu\text{m})^2/\text{s}$ and $Q_{gg}/R = 32,100 \text{ K}$ in the temperature range of 1050 to 1300 K. The grain size variation along the centerline of the workpiece in the deformation zone, after the correction for grain growth, is also presented in Fig. 11. As seen in the figure, the corrected grain size is very close to the desired value of 26 μm .

5. Summary and Conclusions

A two-stage approach for optimal design of metal forming processes has been presented. The first stage involves determining an optimal material deformation path based on models for microstructural development, and the second stage involves determining the optimal process parameters that will impose the desired deformation path on selected areas of a workpiece.

The development uses equations developed by Yada et al. (Ref 13, 14) for dynamic recrystallization of plain carbon steel for the first stage to obtain an optimal material deformation path such that the final grain size is maintained at 26 μm . This trajectory determination was performed via minimization of a cost function which included costs related to both final states and the trajectory followed by the material during processing. In the second stage, a geometric mapping was utilized to develop an extrusion die profile that would deliver the optimal trajectory computed in the first stage. This methodology suggests that using the same die shape, the grain size can be controlled through changes in initial billet temperature and ram velocity for the round-to-round extrusion case.

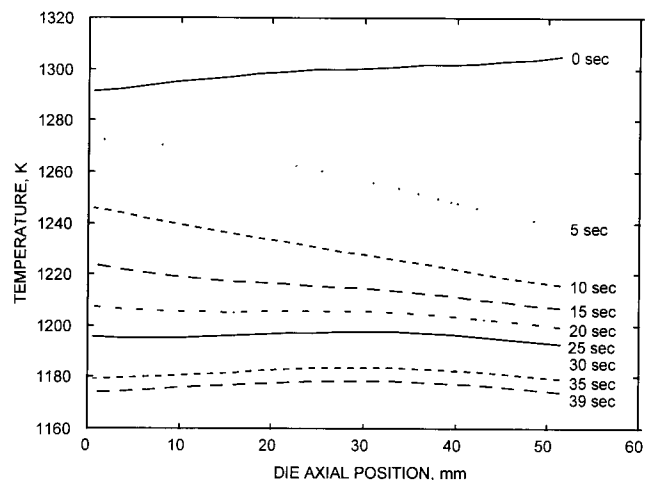


Fig. 12 Simulated temperature distribution along die centerline during air cooling period

A validation experiment was performed by utilizing the extrusion die geometry obtained in the second stage. After correction for static grain growth, the grain size variation within the deformation zone of a partially extruded billet was found to agree with the desired grain size.

Acknowledgments

Support for this research was provided by the Materials Process Design Branch, Materials Directorate, Wright Laboratory, Wright-Patterson Air Force Base. UES, Inc. and Austral Engineering and Software, Inc. participated in this effort as part of a Small Business Innovative Research Program. S. Venugopal is thankful to the National Research Council, U.S.A., for their support. R. Srinivasan would like to acknowledge support from AFOSR through the Summer Faculty Research Program.

References

1. D.E. Kirk, *Optimal Control Theory: An Introduction*, Prentice-Hall, 1970
2. J.J. Jonas, C.M. Sellars, and M. Tegart, Strength and Structure under Hot Working, *Metall. Rev.*, Vol 14 (No. 1), 1969
3. C.M. Sellars, Recrystallization of Metals during Hot Deformation, *Philos. Trans. Roy. Soc.*, Vol 288 (No. 147), 1978
4. H.J. McQueen and J.J. Jonas, Recovery and Recrystallization during High Temperature Deformation, *Treatise on Materials Science and Technology*, Vol 6, *Plastic Deformation of Materials*, Academic Press, 1975, p 393-493
5. W. Roberts, Dynamic Changes That Occur during Hot Working and Their Significance Regarding Microstructural Development and Hot Workability, *Deformation, Processing, and Structure*, G. Krauss, Ed., ASM International, 1984, p 109-184
6. J.C. Malas, "Methodology for Design and Control of Thermomechanical Processes," Ph.D. dissertation, Ohio University, 1991
7. J.C. Malas and V. Seetharaman, Use of Material Behavior Models in the Development of Process Control Strategies, *JOM*, Vol 44 (No. 6), 1992
8. H.J. Frost and M.F. Ashby, *Deformation Maps*, Pergamon Press, 1982
9. R. Raj, Development of a Processing Map for Use in Warm-Forming and Hot-Forming Process, *Metall. Trans. A*, Vol 12, 1981, p 1089

10. W.G. Frazier, Robust Control Techniques for Hot Deformation Processes, *Contributive Research and Development*, Vol 228, SYSTRAN Corp. Final Report, Task 178, Contract F33615-90-C-5944, March 1995
11. A. Kumar, K.P. Rao, E.B. Hawbolt, and I.V. Samarasekera, The Application of Constitutive Equations for Use in the Finite Element Analysis of Hot Rolling Steel, unpublished research, 1987
12. C. Devadas, I.V. Samarasekera, and E.B. Hawbolt, The Thermal and Metallurgical State of Steel Strip during Hot Rolling, Part III: Microstructural Evolution, *Metall. Trans. A*, Vol 22A, 1991, p 335-349
13. H. Yada, Prediction of Microstructural Changes and Mechanical Properties in Hot Strip Rolling, *Proc. Int. Symp. Accelerated Cooling of Rolled Steels*, CIM, G.E. Ruddle and A.F. Crawley, Ed., Pergamon Press, 1987, p 105-120
14. T. Senuma and H. Yada, 1986, Proc. 7th Riso Int. Symp. on Metallurgy and Materials Science, M. Suehiro, K. Sato, Y. Tsukano, H. Yada, T. Senuma, and Y. Matsumura, Annealing Processes, Recovery, Recrystallization and Grain Growth, *Trans. Iron Steel Inst. Japan*, Vol 27, 1987, p 439-445
15. G. Vander Voort, in *Metallography, Principles and Practice*, McGraw-Hill, 1984, p 410
16. *Antares Software User Manual*, UES, Inc., 1995